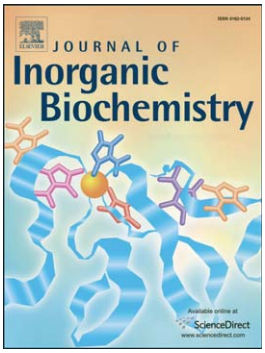

Rhenium(I) Polypyridine Dibenzocyclooctyne Complexes as Phosphorescent Bioorthogonal Probes: Synthesis, Characterization, Emissive Behavior, and Biolabeling Properties

Alex Wing-Tat Choi, Hua-Wei Liu, Kenneth Kam-Wing Lo

PII: S0162-0134(15)00061-6
DOI: doi: 10.1016/j.jinorgbio.2015.02.018
Reference: JIB 9679

To appear in: *Journal of Inorganic Biochemistry*

Received date: 27 October 2014
Revised date: 24 February 2015
Accepted date: 24 February 2015

Please cite this article as: Alex Wing-Tat Choi, Hua-Wei Liu, Kenneth Kam-Wing Lo, Rhenium(I) Polypyridine Dibenzocyclooctyne Complexes as Phosphorescent Bioorthogonal Probes: Synthesis, Characterization, Emissive Behavior, and Biolabeling Properties, *Journal of Inorganic Biochemistry* (2015), doi: 10.1016/j.jinorgbio.2015.02.018

Rhenium(I) Polypyridine Dibenzocyclooctyne Complexes as Phosphorescent Bioorthogonal Probes: Synthesis, Characterization, Emissive Behavior, and Biolabeling Properties

Alex Wing-Tat Choi, Hua-Wei Liu, and Kenneth Kam-Wing Lo*

Department of Biology and Chemistry, City University of Hong Kong, Tat Chee Avenue, Kowloon, Hong Kong (People's Republic of China)

* Corresponding author: E-mail: bhkenlo@cityu.edu.hk; Fax: +852 3442 0522

Abstract: We report the development of rhenium(I) polypyridine complexes appended with a dibenzocyclooctyne (DIBO) moiety as bioorthogonal probes for azide-modified biomolecules. Three phosphorescent rhenium(I) polypyridine DIBO complexes $[Re(N^N)(CO)_3(py\text{-}C6\text{-}DIBO)][CF_3SO_3]$ (py-C6-DIBO = 3-(*N*-(6-(3,4:7,8-dibenzocyclooctyne-5-oxycarbonylamino)hexyl)aminocarbonyl)pyridine; N^N = 1,10-phenanthroline (phen) (**1a**), 3,4,7,8-tetramethyl-1,10-phenanthroline (Me_4-phen) (**2a**), 4,7-diphenyl-1,10-phenanthroline (Ph_2-phen) (**3a**)) and their DIBO-free counterparts $[Re(N^N)(CO)_3(py\text{-}C6\text{-}BOC)][CF_3SO_3]$ (py-C6-BOC = 3-(*N*-(6-(*tert*-butoxycarbonylamino)hexyl)aminocarbonyl)pyridine; N^N = phen (**1b**), Me_4-phen (**2b**), Ph_2-phen (**3b**)) were synthesized and characterized. Upon photoexcitation, all the complexes displayed intense and long-lived yellow triplet metal-to-ligand charge-transfer (^{3}MLCT) ($d\pi(Re) \rightarrow \pi^*(N^N)$) emission. The DIBO complexes underwent facile reactions with benzyl azide in methanol at 298 K with a second-order rate constants (k_2) in the range of 0.077 to 0.091 M^{-1} s^{-1}. As revealed from SDS-PAGE analysis, the DIBO complexes can selectively label azide-modified proteins and the resulting bioconjugates displayed strong phosphorescence upon photoexcitation. Results of inductively coupled plasma mass spectrometry (ICP-MS) and 3-(4,5-dimethylthiazol-2-yl)-2,5-diphenyltetrazolium bromide (MTT) assays indicated that the DIBO complexes accumulated in Chinese Hamster Ovary (CHO) cells with considerable cytotoxic activity. Upon incubation of CHO cells with these complexes, relatively weak intracellular emission was observed. In contrast, upon pretreatment of the cells with 1,3,4,6-tetra-*O*-acetyl-*N*-azidoacetyl-D-mannosamine (Ac_4ManNAz), intense emission was observed from the cell membrane and some internal compartments. The results suggest that the DIBO complexes are promising candidates for imaging azide-labeled biomolecules.

1. Introduction

The discovery of green fluorescent protein enables the visualization of protein dynamics in living systems through a genetic tagging method [1]. However, this strategy is not applicable to the study of non-protein biomolecules such as nucleic acids, glycans, lipids, and small-molecule metabolites. To overcome this limitation, a bioorthogonal chemistry approach has been designed as a versatile method to study these biomolecules in their native environments. A number of chemical reporters and their specific probes for bioorthogonal reactions have been identified and successfully applied in biological studies [2,3]. Among different bioorthogonal reactions, the strain-promoted alkyne-azide cycloaddition (SPAAC) between azide and strained alkyne is one of the most extensively used reactions in bioorthogonal chemistry [4,5]. Azide is a particularly useful handle because of its small size, non-native nature, and inertness toward biomolecules; for example, 1,3,4,6-tetra-*O*-acetyl-*N*-azidoacetyl-D-mannosamine (Ac_4ManNAz) is a very commonly used unnatural sugar derivative [6,7]. Upon cellular uptake, the acetyl groups are removed by carboxyesterases and the mannose derivative is metabolized by glycosyltransferases, and eventually expressed as an end-group of a glycan chain, leaving the azide group unmodified. Thus, the azide group is able to undergo specific reactions with bioorthogonal probes such as a strained alkyne. To date, the design of bioorthogonal probes to trace azide-labeled biomolecules has been focused on affinity tags [8–11], fluorescent organic dyes [12–15], and luminescent quantum dots [16]. Recently, we have prepared iridium(III) dibenzocyclooctyne (DIBO) complexes as the first class of transition metal-based bioorthogonal probes [17]. In view of the interesting photophysical and biological properties of rhenium(I) polypyridine complexes [18], we anticipate that

the modification of these complexes with a DIBO moiety will generate a new class of phosphorescent bioorthogonal reagents for various biological applications. Herein, we report the synthesis and characterization of three phosphorescent rhenium(I) polypyridine DIBO complexes $[Re(N^N)(CO)_3(py\text{-}C6\text{-}DIBO)][CF_3SO_3]$ (py-C6-DIBO = 3-(*N*-(6-(3,4:7,8-dibenzocyclooctyne-5-oxycarbonylamino)hexyl)-aminocarbonyl)pyridine; N^N = 1,10-phenanthroline (phen) (**1a**), 3,4,7,8-tetramethyl-1,10-phenanthroline (Me_4-phen) (**2a**), 4,7-diphenyl-1,10-phenanthroline (Ph_2-phen) (**3a**)) and their DIBO-free counterparts $[Re(N^N)(CO)_3(py\text{-}C6\text{-}BOC)][CF_3SO_3]$ (py-C6-BOC = 3-(*N*-(6-(*tert*-butoxycarbonylamino)hexyl)aminocarbonyl)pyridine; N^N = phen (**1b**), Me_4-phen (**2b**), Ph_2-phen (**3b**)) (Scheme 1). The spectroscopic and photophysical properties of the complexes were studied. The DIBO complexes underwent facile reactions with benzyl azide and the reaction kinetics were investigated. The bioorthogonal labeling properties of these complexes toward azide-modified bovine serum albumin (BSA), human serum albumin (HSA), and apo-transferrin (aTf) were also examined. Additionally, the cellular uptake properties and cytotoxicity of these complexes were studied by inductively coupled plasma mass spectrometry (ICP-MS) and (3-(4,5-dimethylthiazol-2-yl)-2,5-diphenyltetrazolium bromide) (MTT) assays, respectively. Furthermore, the bioorthogonal labeling properties of one of the DIBO complexes were examined using Chinese Hamster Ovary (CHO) cells pretreated with Ac_4ManNAz.

2. Results and Discussion

2.1. Design and Synthesis of Complexes

Regarding the design of the DIBO complexes **1a** – **3a**, the DIBO moiety was attached

to the pyridine ligand through a hexyl spacer-arm to reduce the steric bulkiness of the rhenium(I) polypyridine unit. The pyridine ligand py-C6-DIBO was synthesized from the reaction of 3,4:7,8-dibenzocyclooctyn-5-yl 4-nitrophenyl carbonate with 3-(6-aminohexyl)aminocarbonylpyridine (py-C6-NH_2). The DIBO complexes **1a** – **3a** and the DIBO-free complexes **1b** – **3b** were obtained from the reaction of [Re(N^N)$(CO)_3(CH_3CN)$][CF_3SO_3] with the pyridine ligands py-C6-DIBO and py-C6-BOC, respectively, in refluxing THF. The samples were purified by column chromatography and recrystallization from CH_2Cl_2/diethyl ether. They were characterized by ^{1}H NMR, positive-ion ESI-MS, IR spectroscopy, and microanalysis. All the complexes were stable in air and soluble in most organic solvents such as CH_2Cl_2 and alcohols. One of the basic requirements for luminescent probes is their stability in the medium and environment where they are used [19]. Based on the ESI-MS data, all the complexes in this work remained stable in aqueous solutions (containing 1% DMSO for solubility reasons).

2.2. Photophysical Properties

The electronic absorption spectral data of the complexes are summarized in Table 1. All the complexes displayed intense spin-allowed intraligand (^{1}IL) ($\pi \rightarrow \pi^*$) (N^N and pyridine ligands) absorption bands at ca. 250 – 338 nm and metal-to-ligand charge-transfer (^{1}MLCT) ($d\pi(Re) \rightarrow \pi^*$(N^N)) absorption shoulders at ca. 366 – 394 nm [20–49]. It is noteworthy that the DIBO complexes revealed an additional absorption shoulder at ca. 305 nm, which was assigned to a ($\pi \rightarrow \pi^*$) transition of the DIBO moiety.

Upon photoexcitation, all the complexes showed intense and long-lived green to yellow emission. The photophysical data are summarized in Table 2 and the

emission spectra of the DIBO complexes **1a** – **3a** in CH_3CN at 298 K are shown in Fig. 1. In fluid solutions at 298 K, most of the complexes exhibited reduced emission energy, quantum yields, and lifetimes on changing the solvent from the more polar CH_3CN to the less polar CH_2Cl_2. These findings, together with the dependence of the emission energy on the π* orbital energy level of the N^N ligands, point to an emissive state of triplet metal-to-ligand charge-transfer (^{3}MLCT) (dπ(Re) → π*(N^N)) character. However, the structural features and long emission lifetimes of the Me_4-phen complexes in fluid solutions under ambient conditions (Table 2) suggest the involvement of triplet intraligand (^{3}IL) (π → π*) (Me_4-phen) character in their emissive states.

2.3. Reaction with Benzyl Azide

The azide-targeting properties of the DIBO complexes were examined using benzyl azide as a model substrate (Scheme 2). The SPAAC reaction kinetics of the DIBO complexes with benzyl azide in methanol at 298 K were studied by monitoring the exponential decay of the absorption feature of DIBO at ca. 305 nm and the results are summarized in Table 3. The formation of the triazole complexes was confirmed by electrospray ionization mass spectrometry (ESI-MS) (Table 4) and the plots of the pseudo first-order rate constants (k_{obs}) of the DIBO complexes versus the concentrations of benzyl azide are shown in Fig. 2. The second-order rate constants (k_2) were determined to range from 0.077 to 0.091 M^{-1} s^{-1} (Table 3), which are comparable to those of other DIBO-azide systems such as dibenzocyclooctynol (k_2 = 0.057 M^{-1} s^{-1}) [10] and [Ir(ppy-COOH)$_2$(bpy-TEG-DIBO)][PF_6] (k_2 = 0.069 M^{-1} s^{-1}) [17]. This result reflects that the bulky rhenium(I) polypyridine unit did not adversely affect the reactivity of the DIBO unit due to the long spacer-arm.

2.4. Protein-labeling Studies

The biomolecular targeting properties of the DIBO complexes were studied using complex **1a** as an example. This complex was used to label BSA, HSA, and aTf that had been modified with azidoacetic acid (Scheme 3). The resultant bioconjugates **1-BSA**, **1-HSA**, and **1-aTf** were purified by size exclusion chromatography and ultrafiltration. As revealed from the SDS-PAGE analysis (Fig. 3), the protein-azide conjugates were successfully labeled by the DIBO complexes, giving rise to phosphorescent bands in the gels. The absence of similar bands for the unmodified protein samples confirmed that the labeling originated from the specific reaction between the DIBO moiety of the complexes and the azide units of the conjugates. The photophysical properties of the bioconjugates **1-BSA**, **1-HSA**, and **1-aTf** were studied and the results are summarized in Table 5. All the bioconjugates showed a blue-shifted emission band compared with free complex **1a** in CH_3CN. This observation was ascribed to the increased hydrophobicity of the surroundings of the complex after binding to the proteins. Notably, the emission of all the bioconjugates showed biexponential decay, which is common for biomolecules labeled with phosphorescent transition metal complexes due to their heterogeneous microenvironments on the protein molecule [35,50,51].

2.5. Cellular Uptake Properties and Live-cell Confocal Imaging

The cellular uptake properties of the DIBO complexes were studied using ICP-MS. After incubation with the complexes at 37 ^{o}C for 1 h, an average CHO cell contained 0.32 to 2.07 fmol of rhenium (Table 6), which is comparable to related rhenium(I) polypyridine complexes such as $[Re(phen)(CO)_3(py\text{-}TU\text{-}DPAT)][CF_3SO_3]$ (py-TU-DPAT = 3-(2-(4-hydroxy-3-(2,2'-

dipicolylaminomethyl)phenyl)ethylthioureidyl)pyridine) (2.80 fmol of rhenium) [33] and [Re(phen)$(CO)_3$(py-DA)][PF_6] (py-DA=3-(*N*-(2-amino-5-methoxyphenyl)aminomethyl)pyridine) (0.35 fmol of rhenium) [36]. This result suggests that the modification of rhenium(I) polypyridine complexes with a DIBO moiety did not have substantial effects on their cellular uptake efficiency. The cellular uptake efficiency of the complexes was found to be dependent on the diimine ligands and follow the order: Ph_2-phen > Me_4-phen > phen (Table 6), which is in accordance with the decreasing hydrophobic character of the ligands. The cytotoxicity of the DIBO complexes toward CHO cells over an incubation period of 48 h was investigated using the MTT assay and the IC50 values ranged from 2.94 to 9.55 μM (Table 6). The Ph_2-phen and Me_4-phen complexes exhibited higher cytotoxicity, which is in accordance with their higher uptake efficiency. With reference to the cytotoxic activity of related organometallic rhenium(I) complexes [52], complexes **1a** – **3a** are relatively cytotoxic. Since these complexes are both luminescent and cytotoxic, and exhibit bioorthogonal specificity due to the appended DIBO unit, they can serve as an interesting class of theranostic reagents for a wide range of biological studies.

Laser-scanning confocal microscopy images of live CHO cells treated with the DIBO complex **1a** (5 μM, 1 h) showed that the complex was effectively internalized and localized in the cytoplasmic region (Fig. 4). The cellular uptake pathways of the complexes were studied using the cytoskeletal inhibitor colchicine and ATPase inhibitor potassium nitrate [53]. As revealed from the confocal microscopy images (Fig. 4), the intracellular emission intensity of the CHO cells did not display any significant difference after pretreatment with the two reagents. Additionally, a similar result was found when the cells were incubated at 4 ^{o}C (Fig. 4).

These findings indicate that the DIBO complexes were internalized into CHO cells through an energy-independent passive diffusion pathway.

Since Ac_4ManNAz is metabolically converted by CHO cells to *N*-azidoacetyl sialic acids, which are located on the cell surface [9,13,14], pretreatment of the cells with this reagent is expected to lead to the localization of the complex in the plasma membrane. Confocal microscopy images of Ac_4ManNAz-treated and -untreated CHO cells were very similar upon incubation with complex **1a** for a relatively short incubation time (1 h) (Fig. 5a). This has been attributed to the less efficient labeling of azido sialic acid residues within the cell-surface glycans. This was supported by the ICP-MS measurements which showed that the Ac_4ManNAz pretreatment only slightly increased the rhenium uptake from 0.26 ± 0.02 to 0.35 ± 0.05 fmol per average CHO cell. In other words, the complex did not have sufficient time to react with the surface glycans. Interestingly, upon increasing the incubation time to 24 h, while the CHO cells without pretreatment of Ac_4ManNAz did not show any significant changes in emission intensity, those that were pretreated with Ac_4ManNAz displayed more intense intracellular emission (Fig. 5b), implying increased uptake. This was also confirmed by ICP-MS measurement, which showed that pretreatment with Ac_4ManNAz increased the uptake of rhenium from 0.23 ± 0.02 to 0.57 ± 0.06 fmol per average CHO cell; the dependence of uptake on the incubation time is illustrated in Fig. 6. It is noteworthy that Ac_4ManNAz-treated cells with prolonged incubation time (24 h) exhibited intense emission from the cell membrane and internal compartments which is likely to be Golgi apparatus (Fig. 5b). While the observed membrane labeling was ascribed to the specific reaction of the DIBO unit of complex **1a** with the membrane-bound azido-sialic acid, the enhanced emission of the internal compartments is most likely due to internalization and intracellular trafficking of the

glycans labeled by the luminescent complex. Similar observations of surface-glycan labeling followed by subsequent cellular internalization have been reported for other fluorescent bioorthogonal probes [13] and a related iridium(III) DIBO complex we reported previously. [17]

3. Conclusions

In this work, rhenium(I) polypyridine complexes containing a DIBO moiety were developed as new bioorthogonal probes for azides. Upon photoexcitation, all the complexes displayed intense and long-lived green to yellow emission. The k_2 values for the reactions of the DIBO complexes with benzyl azide were determined to range from 0.077 to 0.091 M^{-1} s^{-1}. Also, these complexes were used to label azide-modified proteins including BSA, HSA, and aTf. The DIBO complexes were found to accumulate in CHO cells with moderate cytotoxicity. Upon incubation of CHO cells with these complexes, relatively weak intracellular emission was observed. In contrast, upon pretreatment of the cells with Ac_4ManNAz, the cell membrane and internal compartments showed intense emission. The observation of membrane labeling is due to the specific reaction of the DIBO unit of complex **1a** with the azido-sialic acid located on the surface of the cells. The enhanced emission of the internal compartments is probably related to the intracellular trafficking of the labeled glycans. Our results indicated that the DIBO complexes are promising reagents for imaging azide-labeled biomolecules. We believe that the bioorthogonal labeling properties of these complexes can be further enhanced by increasing the reactivity of the DIBO moiety and/or decreasing the cellular uptake rate of the complexes. The design of related phosphorescent transition-metal DIBO complexes as bioorthogonal probes for

azide-modified molecules is underway.

4. Experimental Section

4.1. Materials and Synthesis

All solvents were of analytical reagent grade and purified according to standard procedures [54]. Diimine ligands including phen, Me_4-phen, and Ph_2-phen, trifluoroacetic acid, potassium nitrate, colchicines, iodoacetic acid, and *N*-(3-dimethylaminopropyl)-*N*'-ethylcarbodiimide hydrochloride (EDC) were purchased from Acros. Nicotinoyl chloride hydrochloride, sodium azide, *tert*-butyl-*N*-(6-aminohexyl)carbamate hydrochloride, *N*-hydroxybenzotriazole (HOBt), and MTT were obtained from Sigma. Benzyl azide was purchased from Alfa Aesar. BSA (Fraction V, RIA and ELISA Grade), HSA (Fraction V, High Purity), and aTf (Human Plasma) were obtained from Calbiochem. All these chemicals were used without further purification. $[Re(N\text{^}N)(CO)_3(CH_3CN)][CF_3SO_3]$ [55] and 3,4:7,8-dibenzocyclooctyn-5-yl 4-nitrophenyl carbonate [9] were prepared according to reported procedures. All buffer components were of biological grade and used as received. Autoclaved Milli-Q water was used for the preparation of aqueous solutions. CHO cells were obtained from American Type Culture Collection. F12-nutrition mixture, fetal bovine serum (FBS), phosphate buffered saline (PBS) , trypsin-EDTA, Novex® sharp pre-stained protein standard, Ac_4ManNAz, and penicillin/streptomycin were purchased from Invitrogen. The growth medium for cell culture contained F12-nutrition mixture with 10% FBS and 1% penicillin/streptomycin.

***Py-C6-BOC*:** A mixture of nicotinoyl chloride hydrochloride (1.01 g, 5.62 mmol) and *tert*-butyl-*N*-(6-aminohexyl)carbamate hydrochloride (1.42 g, 5.62 mmol) in pyridine

(10 mL) was stirred under an inert atmosphere of nitrogen at room temperature for 24 h. Water (100 mL) was added to quench the reaction, and the product was extracted with CH_2Cl_2 (150 mL × 3). The combined organic layer was dried over $MgSO_4$ and evaporated to dryness yielding a yellow solid, which was purified by column chromatography on silica gel. The desired product was eluted with hexane/ethyl acetate (1:4, *v*/*v*). The solvent was removed under vacuum to afford the product as a white solid. Yield: 766 mg (42%). ^{1}H NMR (300 MHz, CD_3OD, 298 K): δ 8.96 (s, 1H, H2 of pyridine), 8.67 (d, 1H, J = 3.3 Hz, H6 of pyridine), 8.23 (d, 1H, J = 8.1 Hz, H4 of pyridine), 7.56 – 7.52 (m, 1H, H5 of pyridine), 3.41 – 3.30 (t, 2H, J = 6.9 Hz, py-3-CONHCH_2), 3.05 – 3.00 (t, 2H, J = 6.9 Hz, $(CH_3)_3$OCONHCH_2), 1.66 – 1.39 (m, 17H, $CH_2(CH_2)_4CH_2$ and CH_3 of Boc). Positive-ion ESI-MS ion cluster at *m*/*z* 322 $\{M + H^+\}^+$.

***Py-C6-NH$_2$*:** A mixture of py-C6-BOC (478 mg, 1.46 mmol) and trifluoroacetic acid (1 mL) in CH_2Cl_2 (6 mL) was stirred under an inert atmosphere of nitrogen at room temperature for 30 min. The solution was evaporated to dryness yielding a pale yellow solid, which was purified by column chromatography on silica gel. The desired product was eluted with CH_2Cl_2/MeOH (5:1, *v*/*v*). The solvent was removed under vacuum to afford the product as a white solid. Yield: 289 mg (90%). ^{1}H NMR (300 MHz, CD_3OD, 298 K): δ 8.98 (s, 1H, H2 of pyridine), 8.67 (d, 1H, J = 2.4 Hz, H6 of pyridine), 8.25 (d, 1H, J = 7.8 Hz, H4 of pyridine), 7.54 (dd, 1H, J = 7.8 and 2.4 Hz, H5 of pyridine), 3.43 – 3.30 (m, 2H, py-3-CONHCH_2), 2.94 (t, 2H, J = 7.5 Hz, NH_2CH_2), 1.72 – 1.42 (m, 8H, $CH_2(CH_2)_4CH_2$). Positive-ion ESI-MS ion cluster at *m*/*z* 222 $\{M + H^+\}^+$.

***Py-C6-DIBO*:** A mixture of py-C6-NH_2 (150 mg, 0.69 mmol), 3,4:7,8-dibenzocyclooctyn-5-yl 4-nitrophenyl carbonate (261 mg, 0.69 mmol), and

triethylamine (2 mL) in CH_2Cl_2 (15 mL) was stirred under an inert atmosphere of nitrogen at room temperature for 4 h. The solution was evaporated to dryness yielding a pale grey solid, which was purified by column chromatography on silica gel. The desired product was eluted with CH_2Cl_2/MeOH (5:1, *v*/*v*). The solvent was removed under vacuum to afford the product as a white solid. Yield: 231 mg (73%). ^{1}H NMR (300 MHz, $CDCl_3$, 298 K): δ 8.96 (s, 1H, H2 of pyridine), 8.61 (d, 1H, J = 5.1 Hz, H6 of pyridine), 8.00 (d, 1H, J = 7.8 Hz, H4 of pyridine), 7.44 (d, 1H, J = 7.5 Hz, H5 of pyridine), 7.34 – 7.20 (m, 8H, C_6H_4 of DIBO), 7.05 (br, 1H, py-3-CONH), 5.44 – 5.42 (m, 2H, OCONH and OCH of DIBO), 3.34 – 3.23 (m, 2H, py-3-CONHCH_2), 3.18 – 3.10 (m, 3H, OCONHCH_2 of DIBO and CH_2 of DIBO), 2.83 (dd, 1H, J = 15 and 3.9 Hz, CH_2 of DIBO), 1.50 – 1.22 (m, 8H, $CH_2(CH_2)_4CH_2$). Positive-ion ESI-MS ion cluster at m/z 469 $\{M + H^+\}^+$.

***[Re(N^N)(CO)$_3$(py-C6-DIBO)][CF$_3$SO$_3$] (N^N = phen (1a), Me$_4$-phen (2a), Ph$_2$-phen (3a))*:** A mixture of [Re(N^N)(CO)$_3$(CH$_3$CN)][CF$_3$SO$_3$] (0.13 mmol) and py-C6-DIBO (63 mg, 0.13 mmol) in THF (30 mL) was refluxed under an inert atmosphere of nitrogen for 12 h. Subsequent recrystallization of the complex from CH_2Cl_2/diethyl ether resulted in the formation of the complex as yellow crystals. Complex **1a**. Yield: 100 mg (70%). ^{1}H NMR (300 MHz, CD_3OD, 298 K): δ 9.75 (d, 2H, J = 5.1 Hz, H2 and H9 of phen), 8.91 (d, 2H, J = 8.4 Hz, H4 and H7 of phen), 8.62 – 8.59 (m, 2H, H2 and H6 of pyridine), 8.21 – 8.17 (m, 4H, H3, H5, H6, and H8 of phen), 8.08 – 8.07 (m, 1H, H4 of pyridine), 7.49 (d, 1H, J = 7.8 Hz, H5 of pyridine), 7.37 – 7.23 (m, 8H, C_6H_4 of DIBO), 5.27 – 5.26 (m, 1H, OCH of DIBO), 3.32 – 3.06 (m, 5H, CH_2 and OCONHCH_2 of DIBO and py-3-CONHCH_2), 2.74 (dd, 1H, J = 15 and 3.9 Hz, CH_2 of DIBO), 1.51 – 1.28 (m, 8H, $CH_2(CH_2)_4CH_2$). IR (KBr) ν/cm^{-1}: 3447 (m, N–H), 2031 (s, C≡O), 1919 (s, C≡O), 1161 (m, $CF_3SO_3^-$), 1030 (m,

$CF_3SO_3^-$). Positive-ion ESI-MS ion cluster at *m*/*z* 918 $\{M - CF_3SO_3^-\}^+$. Elemental analysis calcd (%) for $C_{45}H_{37}N_5O_9SF_3Re \cdot 1.5H_2O \cdot 0.5(CH_3CH_2)_2O$: C 49.91; H 4.01; N 6.19. Found: C 49.85; H 4.03; N 6.43. Complex **2a**. Yield: 80 mg (53%). ^{1}H NMR (300 MHz, CD_3OD, 298 K): δ 9.48 (s, 2H, H2 and H9 of Me_4-phen), 8.66 – 8.60 (m, 2H, H2 and H6 of pyridine), 8.37 (s, 2H, H5 and H6 of Me_4-phen), 8.10 (d, *J* = 6.0 Hz, H4 of pyridine), 7.52 – 7.04 (m, 9H, C_6H_4 of DIBO and H5 of pyridine), 5.27 (s, 1H, OCH of DIBO), 3.21 – 3.06 (m, 5H, CH_2 and OCONHCH_2 of DIBO and py-3-CONHCH_2), 2.86 (s, 6H, CH_3 at C4 and C7 of Me_4-phen), 2.74 – 2.70 (m, 7H, CH_2 of DIBO and CH_3 at C3 and C8 of Me_4-phen), 1.53 – 1.35 (m, 8H, $CH_2(CH_2)_4CH_2$). IR (KBr) ν/cm^{-1}: 3447 (m, N–H), 2031 (s, C≡O), 1918 (s, C≡O), 1161 (m, $CF_3SO_3^-$), 1030 (m, $CF_3SO_3^-$). Positive-ion ESI-MS ion cluster at *m*/*z* 974 $\{M - CF_3SO_3^-\}^+$. Elemental analysis calcd (%) for $C_{49}H_{45}N_5O_9SF_3Re \cdot 1.5H_2O$: C 51.17; H 4.21; N 6.09. Found: C 50.79; H 4.21; N 6.40. Complex **3a**. Yield: 105 mg (64%). ^{1}H NMR (300 MHz, CD_3OD, 298 K): δ 9.83 – 9.81 (m, 2H, H2 and H9 of Ph_2-phen), 8.75 – 8.74 (m, 2H, H2 and H6 of pyridine), 8.20 – 8.15 (m, 5H, H4 of pyridine and H3, H5, H6, and H8 of Ph_2-phen), 7.73 – 7.63 (m, 10H, C_6H_5 of Ph_2-phen), 7.50 – 7.25 (m, 9H, C_6H_4 of DIBO and H5 of pyridine), 5.24 (s, 1H, OCH of DIBO), 3.24 – 3.07 (m, 5H, CH_2 and OCONHCH_2 of DIBO and py-3-CONHCH_2), 2.74 (d, 1H, *J* = 11 Hz, CH_2 of DIBO), 1.54 – 1.32 (m, 8H, $CH_2(CH_2)_4CH_2$). IR (KBr) ν/cm^{-1}: 3448 (m, N–H), 2032 (s, C≡O), 1920 (s, C≡O), 1158 (m, $CF_3SO_3^-$), 1030 (m, $CF_3SO_3^-$). Positive-ion ESI-MS ion cluster at *m*/*z* 1071 $\{M - CF_3SO_3^-\}^+$. Elemental analysis calcd (%) for $C_{57}H_{45}N_5O_9SF_3Re \cdot 2H_2O$: C 54.54; H 3.93; N 5.58. Found: C 54.70; H 4.22; N 5.82.

***[Re(N^N)(CO)$_3$(py-C6-BOC)][CF$_3$SO$_3$] (N^N = phen (1b), Me$_4$-phen (2b), Ph$_2$-phen (3b))*:** A mixture of [Re(N^N)(CO)$_3$(CH$_3$CN)][CF$_3$SO$_3$] (0.13 mmol) and py-

C6-BOC (42 mg, 0.13 mmol) in THF (30 mL) was refluxed under an inert atmosphere of nitrogen for 12 h. Subsequent recrystallization of the complex from CH_2Cl_2/diethyl ether resulted in the formation of the complex as yellow crystals. Complex **1b**. Yield: 85 mg (71%). ^{1}H NMR (300 MHz, CD_3OD, 298 K): δ 9.76 (d, 2H, J = 5.1 Hz, H2 and H9 of phen), 8.95 (d, 2H, J = 8.4 Hz, H4 and H7 of phen), 8.65 – 8.60 (m, 2H, H2 and H6 of pyridine), 8.24 – 8.15 (m, 5H, H3, H5, H6, and H8 of phen and H4 of pyridine), 7.39 – 7.35 (m, 1H, H5 of pyridine), 3.25 (t, 2H, J = 7.2 Hz, py-3-CONHCH_2), 3.00 (t, 2H, J = 6.6 Hz, NHCH_2), 1.51 – 1.30 (m, 17H, $CH_2(CH_2)_4CH_2$ and CH_3 of Boc). IR (KBr) ν/cm^{-1}: 3443 (m, N–H), 2031 (s, C≡O), 1923 (s, C≡O), 1165 (m, $CF_3SO_3^-$), 1031 (m, $CF_3SO_3^-$). Positive-ion ESI-MS ion cluster at m/z 772 $\{M - CF_3SO_3^-\}^+$. Elemental analysis calcd (%) for $C_{33}H_{35}N_5O_9SF_3Re{\cdot}H_2O$: C 42.21; H 3.97; N 7.46. Found: C 42.46; H 4.24; N 7.34. Complex **2b**. Yield: 71 mg (56%). ^{1}H NMR (300 MHz, CD_3OD, 298 K): δ 9.46 (s, 2H, H2 and H9 of Me_4-phen), 8.67 – 8.61 (m, 2H, H2 and H6 of pyridine), 8.41 (s, 2H, H5 and H6 of Me_4-phen), 8.18 (d, J = 5.7 Hz, H4 of pyridine), 7.38 (t, J = 4.5 Hz, H5 of pyridine), 3.30 – 3.26 (m, 2H, py-3-CONHCH_2), 3.10 – 2.98 (m, 2H, NHCH_2), 2.91 (s, 6H, CH_3 at C4 and C7 of Me_4-phen), 2.77 (s, CH_3 at C3 and C8 of Me_4-phen), 1.54 – 1.34 (m, 17H, $CH_2(CH_2)_4CH_2$ and CH_3 of Boc). IR (KBr) ν/cm^{-1}: 3463 (m, N–H), 2032 (s, C≡O), 1919 (s, C≡O), 1162 (m, $CF_3SO_3^-$), 1031 (m, $CF_3SO_3^-$). Positive-ion ESI-MS ion cluster at m/z 828 $\{M - CF_3SO_3^-\}^+$. Elemental analysis calcd (%) for $C_{37}H_{43}N_5O_9SF_3Re{\cdot}H_2O{\cdot}0.5CH_3OH$: C 44.55; H 4.69; N 6.93. Found: C 44.69; H 4.97; N 7.29. Complex **3b**. Yield: 60 mg (43%). ^{1}H NMR (300 MHz, CD_3OD, 298 K): δ 9.81 – 9.80 (m, 2H, H2 and H9 of Ph_2-phen), 8.77 – 8.73 (m, 2H, H2 and H6 of pyridine), 8.22 – 8.18 (m, 5H, H4 of pyridine and H3, H5, H6, and H8 of Ph_2-phen),

7.68 – 7.47 (m, 11H, C_6H_5 of Ph_2-phen and H5 of pyridine), 3.34 – 3.30 (m, 2H, py-3-CONHCH_2), 3.05 – 2.98 (m, 2H, NHCH_2), 1.53 – 1.32 (m, 17H, $CH_2(CH_2)_4CH_2$ and CH_3 of Boc). IR (KBr) ν/cm^{-1}: 3448 (m, N–H), 2033 (s, C≡O), 1920 (s, C≡O), 1162 (m, $CF_3SO_3^-$), 1030 (m, $CF_3SO_3^-$). Positive-ion ESI-MS ion cluster at *m*/*z* 924 {M – $CF_3SO_3^-$}$^+$. Elemental analysis calcd (%) for $C_{45}H_{43}N_5O_9SF_3Re{\cdot}3H_2O$: C 47.95; H 4.38; N 6.21. Found: C 48.17; H 4.33; N 6.56.

4.2. Instrumentation and Methods

^{1}H NMR spectra were recorded on a Varian Mercury 300 MHz NMR spectrometer at 298 K. Positive-ion ESI mass spectra were recorded on a Perkin-Elmer Sciex API 365 mass spectrometer. IR spectra were recorded on a Perkin-Elmer 1600 series FT-IR spectrophotometer. Elemental analyses were carried out on a Vario EL III CHN elemental analyzer. Electronic absorption and steady-state emission spectra were recorded on a Hewlett-Packard 8453 diode array spectrophotometer and a SPEX FluoroLog 3-TCSPC spectrophotometer equipped with a Hamamatsu R928 PMT detector, respectively. Emission lifetimes were measured in the Fast MCS lifetime mode with a NanoLED N-375 as the excitation source. All the solutions for photophysical studies were degassed with at least four successive freeze-pump-thaw cycles and stored in a 10-cm^3 round-bottomed flask equipped with a sidearm 1-cm fluorescence cuvette and sealed from the atmosphere by a Rotaflo HP6/6 quick-release Teflon stopper. Luminescence quantum yields were measured by the optically dilute method [56] using a degassed CH_3CN solution of [Re(phen)(CO)$_3$(pyridine)][CF_3SO_3] (Φ_{em} = 0.18, λ_{ex} = 355 nm) as the standard solution [57]. Details on MTT assays and ICP-MS have been reported previously [33,58].

4.3. Kinetics Studies

Kinetic experiments for the reactions of the DIBO complexes with benzyl azide were performed under pseudo first-order conditions. The DIBO complexes (20 μM) were mixed in a 1:100, 1:150, 1:200, or 1:250 molar ratio with benzyl azide in MeOH at 298 K and the reactions were monitored by UV-Visible (UV-Vis) spectroscopy at ca. 305 nm. The k_{obs} values were determined by fitting the experimental data to the first-order rate equation, $[A] = [A]_o e^{-kt}$. The k_2 values were determined by plotting k_{obs} versus [benzyl azide] and the rate constant corresponds to the determined slope.

4.4. Preparation of Azidoacetic Acid

A mixture of iodoacetic acid (1.86 g, 10 mmol) and sodium azide (1.43 g, 22 mmol) in H_2O (25 mL) was stirred slowly in dark at room temperature for 48 h. The mixture was acidified with 1 M HCl and the solution was extracted with diethyl ether (50 mL × 3). The organic phase was washed with saturated $NaHSO_3$ and then dried over $MgSO_4$. The solvent was evaporated to dryness yielding azidoacetic acid as a yellow oil. Yield: 483 mg (48%). ^{1}H NMR (300 MHz, $CDCl_3$, 298 K): δ 3.96 (s, 2H, CH_2).

4.5. Modification of BSA, HSA, and aTf with Azidoacetic Acid

A mixture of the protein (BSA, HSA, or aTf) (0.10 μmol), azidoacetic acid (450.0 μg, 4.5 μmol), EDC (1.4 mg, 9.0 μmol), and HOBt (1.2 mg, 9.0 μmol) in 50 mM potassium phosphate buffer at pH 7.4 (500 μL) was stirred in the dark at room temperature for 24 h. The solution was loaded onto a PD-10 size exclusion column. Volume fractions between 2.5 and 5.0 mL were collected. Finally, the bioconjugates were washed successively with potassium phosphate buffer using an YM-50 centricon, concentrated to 1.0 mL, and stored at 4 °C.

4.6. Labeling of Azide-modified Proteins

In a typical reaction, complex **1a** (0.21 mg, 0.20 μmol) in anhydrous DMSO (20 μL) was added to the azide-modified BSA, HSA, or aTf (0.02 μmol) dissolved in 50 mM potassium phosphate buffer at pH 7.4 (980 μL). The solution was stirred in the dark at room temperature for 24 h. Any precipitate was removed by centrifugation and the supernatant was loaded onto a PD-10 size exclusion column. The first colored band was collected and washed successively with potassium phosphate buffer using an YM-50 centricon, concentrated to 1.0 mL, and stored at 4 °C.

4.7. Live-cell Confocal Microscopy and Bioorthogonal Imaging in CHO Cells

CHO cells in growth medium were seeded on a sterilized coverslip in a 60-mm tissue culture dish and grown at 37 °C under a 5% CO_2 atmosphere for 48 h. The culture medium was then removed and replaced with medium/DMSO (99:1, *v*/*v*) containing complex **1a** (5 μM). After incubation for 1 h, the medium was removed and the cell layer was washed gently with PBS (1 mL × 3). The coverslip was mounted onto a sterilized glass slide and then imaged using a Leica TCS SPE confocal microscope. In the bioorthogonal imaging experiments, the cells were pretreated with Ac_4ManNAz (50 μM) in growth medium for 72 h, and finally washed with PBS (1 mL × 3).

5. Abbreviations

Ac_4ManNAz	1,3,4,6-tetra-*O*-acetyl-*N*-azidoacetyl-D-mannosamine
aTf	apo-transferrin
BSA	bovine serum albumin

CHO	Chinese Hamster Ovary
DIBO	dibenzocyclooctyne
HSA	human serum albumin
IL	intraligand
Me_4-phen	3,4,7,8-tetramethyl-1,10-phenanthroline
MLCT	metal-to-ligand charge-transfer
Ph_2-phen	4,7-diphenyl-1,10-phenanthroline
phen	1,10-phenanthroline
py-C6-BOC	3-(*N*-(6-(*tert*-butoxycarbonylamino)hexyl)aminocarbonyl)pyridine
py-C6-DIBO	3-(*N*-(6-(3,4:7,8-dibenzocyclooctyne-5-oxycarbonylamino)hexyl)aminocarbonyl)pyridine
SPAAC	strain-promoted alkyne-azide cycloaddition

Supporting information for this article is available on the WWW under http://dx.doi.org/10.1016/j.jinorgbio.2014.xx.xxx

Acknowledgements

We thank the Hong Kong Research Grants Councils (Project No. CityU 102212) and City University of Hong Kong (Project No. 9667090) for financial support. We thank Mr. Tat-Ming Wong for his involvement in the early stage of this project. A.W.-T.C. acknowledges the receipt of a Postgraduate Studentship, a Research Tuition Scholarship, and a Student Research Excellence Award administered by City University of Hong Kong.

References

[1] G. U. Nienhaus, Angew. Chem. Int. Ed. 47 (2008) 8992-8994.

[2] C. P. Ramil, Q. Lin, Chem. Commun. 49 (2013) 11007-11022.

[3] D. M. Patterson, L. A. Nazarova, J. A. Prescher, ACS Chem. Biol. 9 (2014) 592-605.

[4] E. M. Sletten, C. R. Bertozzi, Angew. Chem. Int. Ed. 48 (2009) 6974-6998.

[5] E. M. Sletten, C. R. Bertozzi, Acc. Chem. Res. 44 (2011) 666-676.

[6] A. Helenius, M. Aebi, Science 291 (2001) 2364-2369.

[7] J. A. Prescher, D. H. Dube, C. R. Bertozzi, Nature 430 (2004) 873-877.

[8] E. Saxon, C. R. Bertozzi, Science 287 (2000) 2007-2010.

[9] X. Ning, J. Guo, M. A. Wolfert, G.-J. Boons, Angew. Chem. Int. Ed. 47 (2008) 2253-2255.

[10] A. A. Poloukhtine, N. E. Mbua, M. A. Wolfert, G.-J. Boons, V. V. Popik, J. Am. Chem. Soc. 131 (2009) 15769-15776.

[11] J. Dommerholt, S. Schmidt, R. Temming, L. J. A. Hendriks, F. P. J. T. Rutjes, J. C. M. van Hest, D. J. Lefeber, P. Friedl, F. L. van Delft, Angew. Chem. Int. Ed. 49 (2010) 9422-9452.

[12] P. V. Chang, J. A. Prescher, M. J. Hangauer, C. R. Bertozzi, J. Am. Chem. Soc. 129 (2007) 8400-8401.

[13] J. M. Baskin, J. A. Prescher, S. T. Laughlin, N. J. Agard, P. V. Chang, I. A. Miller, A. Lo, J. A. Codelli, C. R. Bertozzi, Proc. Natl. Acad. Sci. U. S. A. 104 (2007) 16793-16797.

[14] J. C. Jewett, E. M. Sletten, C. R. Bertozzi, J. Am. Chem. Soc. 132 (2010) 3688-3690.

[15] S. T. Laughlin, J. M. Baskin, S. L. Amacher, C. R. Bertozzi, Science 320 (2008)

664-667.

[16] A. Bernardin, A. Cazet, L. Guyon, P. Delannoy, F. Vinet, D. Bonnaffé, I. Texier, Bioconjugate Chem. 21 (2010) 583-588.

[17] K. K.-W. Lo, B. T.-N. Chan, H.-W. Liu, K. Y. Zhang, S. P.-Y. Li, T. S.-M. Tang, Chem. Commun. 49 (2013) 4271-4273.

[18] K. K.-W. Lo, K. Y. Zhang, S. P.-Y. Li, Eur. J. Inorg. Chem. (2011) 3551-3568.

[19] A. Leonidova, V. Pierroz, L. A. Adams, N. Barlow, S. Ferrari, B. Graham, G. Gasser, ACS Med. Chem. Lett. 5 (2014) 809-814.

[20] E. Ferri, D. Donghi, M. Panigati, G. Prencipe, L. D'Alfonso, I. Zanoni, C. Baldoli, S. Maiorana, G. D'Alfonso, E. Licandro, Chem. Commun. 46 (2010) 6255-6257.

[21] C. Mari, M. Panigati, L. D'Alfonso, I. Zanoni, D. Donghi, L. Sironi, M. Collini, S. Maiorana, C. Baldoli, G. D'Alfonso, E. Licandro, Organometallics 31 (2012) 5918-5928.

[22] L. Raszeja, A. Maghnouj, S. Hahn, N. Metzler-Nolte, ChemBioChem 12 (2011) 371-376.

[23] G. Gasser, S. Neumann, I. Ott, M. Seitz, R. Heumann, N. Metzler-Nolte, Eur. J. Inorg. Chem. (2011) 5471-5478.

[24] G. Gasser, A. Pinto, S. Neumann, A. M. Sosniak, M. Seitz, K. Merz, R. Heumann, N. Metzler-Nolte, Dalton Trans. 41 (2012) 2304-2313.

[25] A. Leonidova, V. Pierroz, R. Rubbiani, J. Heier, S. Ferrari, G. Gasser, Dalton Trans. 43 (2014) 4287-4294.

[26] I. Kitanovic, S. Can, H. Alborzina, A. Kitanovic, V. Pierroz, A. Leonidvoa, A. Pinto, B. Spingler, S. Ferrari, R. Molteni, A. Steffen, N. Metzler-Nolte, S. Wölfl, G. Gasser, Chem. Eur. J. 20 (2014) 2496-2507.

[27] A. E. Pierri, A. Pallaoro, G. Wu, P. C. Ford, J. Am. Chem. Soc. 134 (2012) 18197-18200.

[28] N. Voila-Villegas, A. E. Rabideau, J. Cesnavicious, J. Zubieta, R. P. Doyle, ChemMedChem 3 (2008) 1387-1397.

[29] N. Viola-Villegas, A. E. Rabideau, M. Bartholoma, J. Zubieta, R. P. Doyle, J. Med. Chem. 52 (2009) 5253-5261.

[30] A. J. Amoroso, R. J. Arthur, M. P. Coogan, J. B. Court, V. Fernández-Moreira, A. J. Hayes, D. Lloyd, C. Millet, S. J. A. Pope, New J. Chem. 32 (2008) 1097-1102.

[31] F. L. Thorp-Greenwood, M. P. Coogan, L. Mishra, N. Kumari, G. Rai, S. Saripella, New J. Chem. 36 (2012) 64-72.

[32] V. Fernández-Moreira, M. L. Ortego, C. F. Williams, M. P. Coogan, M. D. Villacampa, M. C. Gimeno, Organometallics 31 (2012) 5950-5957.

[33] M.-W. Louie, H.-W. Liu, M. H.-C. Lam, T.-C. Lau, K. K.-W. Lo, Organometallics 28 (2009) 4297-4307.

[34] M.-W. Louie, H.-W. Liu, M. H.-C. Lam, Y.-W. Lam, K. K.-W. Lo, Chem. Eur. J. 17 (2011) 8304-8308.

[35] A. W.-T. Choi, M.-W. Louie, S. P.-Y. Li, H.-W. Liu, B. T.-N. Chan, T. C.-Y. Lam, A. C.-C. Lin, S.-H. Cheng, K. K.-W. Lo, Inorg. Chem. 51 (2012) 13289-13302.

[36] A. W.-T. Choi, V. M.-W. Yim, H.-W. Liu, K. K.-W. Lo, Chem. Eur. J. 20 (2014) 9633-9642.

[37] S. L. Mecklenburg, K. A. Opperman, P. Chen, T. J. Meyer, J. Phys. Chem. 100 (1996) 15145-15151.

[38] R. López, A. M. Leiva, F. Zuloaga, B. Loeb, E. Norambuena, K. M. Omberg, J.

R. Schoonover, D. Striplin, M. Devenney, T. J. Meyer, Inorg. Chem. 38 (1999) 2924-2930.

[39] A. Juris, S. Campagna, I. Bidd, J.-M. Lehn, R. Ziessel, Inorg. Chem. 27 (1988) 4007-4011.

[40] R. Ziessel, A. Juris, M. Venturi, Chem. Commun. (1997) 1593-1594.

[41] W. B. Connick, A. J. Di Bilio, M. G. Hill, J. R. Winkler, H. B. Gray, Inorg. Chim. Acta 240 (1995) 169-173.

[42] O. S. Wenger, L. M. Henling, M. W. Day, J. R. Winkler, H. B. Gray, Inorg. Chem. 43 (2004) 2043-2048.

[43] V. W.-W. Yam, V. C.-Y. Lau, L.-X. Wu, J. Chem. Soc., Dalton Trans. (1998) 1461-1468.

[44] S. C.-F. Lam, V. W.-W. Yam, K. M.-C. Wong, E. C.-C. Cheng, N. Zhu, Organometallics 24 (2005) 4298-4305.

[45] X.-Q. Guo, F. N. Castellano, L. Li, H. Szmacinski, J. R. Lakowicz, J. Sipior, Anal. Biochem. 254 (1997) 179-186.

[46] Y. Shen, B. P. Maliwal, J. R. Lakowicz, J. Fluoresc. 11 (2001) 315-318.

[47] A. J. Lees, Chem. Rev. 87 (1987) 711-743.

[48] T. G. Kotch, A. J. Lees, S. J. Fuerniss, K. I. Papathomas, R. W. Snyder, Inorg. Chem. 32 (1993) 2570-2575.

[49] S.-S. Sun, A. J. Lees, Organometallics 21 (2002) 39-49.

[50] K. K.-W. Lo, D. C.-M. Ng, C.-K. Chung, Organometallics 20 (2001) 4999-5001.

[51] S.-K. Leung, K. Y. Kwok, K. Y. Zhang, K. K.-W. Lo, Inorg. Chem. 49 (2010) 4984-4995.

[52] A. Leonidova, G. Gasser, ACS Chem. Biol. 9 (2014) 2180-2193.

[53] E. Reaven, L. Tsai, S. Azhar, J. Biol. Chem. 271 (1996) 16208-16217.

[54] D. D. Perrin, W. L. F. Armarego, Purification of Laboratory Chemicals, 3rd ed., Pergamon Press, New York, 1988.

[55] K. K.-W. Lo, W.-K. Hui, Inorg. Chem. 44 (2005) 1992-2002.

[56] J. N. Demas, G. A. Crosby, J. Phys. Chem. 75 (1971) 991-1024.

[57] L. Wallace, D. P. Rillema, Inorg. Chem. 32 (1993) 3836-3843.

[58] K. K.-W. Lo, K. Y. Zhang, S.-K. Leung, M.-C. Tang, Angew. Chem. Int. Ed. 47 (2008) 2213-2216.

Table 1

Electronic absorption spectral data of the rhenium(I) polypyridine complexes at 298 K.

complex	solvent	λ_{abs} [nm] (ε [M^{-1} cm^{-1}])
1a	CH_2Cl_2	257 sh (30 365), 277 (38 725), 288 sh (34 460), 306 (25 385), 334 sh (5940), 375 sh (4005)
	CH_3CN	259 sh (31 165), 274 (41 920), 285 sh (38 860), 304 (29 245), 330 sh (6655), 367 sh (3970)
1b	CH_2Cl_2	257 sh (27 585), 277 (29 790), 295 sh (16 155), 334 sh (6140), 380 sh (4085)
	CH_3CN	254 sh (22 710), 274 (26 840), 290 sh (15 775), 325 sh (6225), 368 sh (3560)
2a	CH_2Cl_2	254 (33 715), 282 (46 375), 306 (32 055), 328 sh (10 840), 369 sh (4245)
	CH_3CN	250 (34 945), 286 (46 340), 304 (33 300), 320 sh (12 260), 366 sh (3710)
2b	CH_2Cl_2	251 (30 520), 282 (33 815), 325 sh (12 610), 373 sh (4305)
	CH_3CN	247 (33 530), 280 (35 020), 313 sh (14 755), 366 sh (3880)
3a	CH_2Cl_2	276 sh (44 430), 289 (57 335), 304 sh (46 980), 338 sh (16 265), 384 sh (8970)
	CH_3CN	264 sh (37 375), 288 (58 395), 303 sh (45 995), 334 sh (16 780), 382 sh (7995)
3b	CH_2Cl_2	271 sh (34 445), 294 (49 710), 337 sh (20 650), 394 sh (9245)
	CH_3CN	258 sh (35 105), 291 (51 485), 334 sh (20 495), 386 sh (9295)

Table 2

Photophysical data of the rhenium(I) polypyridine complexes at 298 K.

complex	solvent	λ_{em} [nm]	τ_o [μs]	Φ_{em}
1a	CH_2Cl_2	528	1.86	0.45
	CH_3CN	545	1.24	0.11
1b	CH_2Cl_2	528	2.55	0.63
	CH_3CN	545	1.68	0.15
2a	CH_2Cl_2	492,[a] 510	3.03	0.07
	CH_3CN	485,[a] 512	4.57	0.03
2b	CH_2Cl_2	490,[a] 511	9.27	0.28
	CH_3CN	486,[a] 512	8.27	0.06
3a	CH_2Cl_2	542	7.24	0.30
	CH_3CN	556	4.20	0.09
3b	CH_2Cl_2	542	7.19	0.24
	CH_3CN	556	4.43	0.09

[a] Shoulders.

Table 3

The k_2 values for the DIBO complexes upon reaction with benzyl azide in MeOH at 298 K.

complex	k_2 [M^{-1} s^{-1}]
1a	0.077
2a	0.085
3a	0.091

Table 4

ESI-mass spectrometry data for the DIBO complexes after the reactions with benzyl azide in MeOH at 298 K.

complex	formula for $[M - CF_3SO_3^-]^+$	mass calculated for $[M - CF_3SO_3^-]^+$	mass found for $[M - CF_3SO_3^-]^+$
1a	$ReC_{51}H_{44}N_8O_6^+$	1051.3	1051.5
2a	$ReC_{55}H_{52}N_8O_6^+$	1107.4	1107.6
3a	$ReC_{63}H_{52}N_8O_6^+$	1203.4	1203.9

Table 5

Photophysical data of conjugates **1-BSA**, **1-HSA**, and **1-aTf** in degassed 50 mM potassium phosphate buffer pH 7.4 at 298 K.

conjugate	λ_{em}/nm	τ_o/μs	Φ_{em}
1-BSA	535	0.96 (82%), 2.75 (18%)	0.089
1-HSA	534	0.91 (77%), 2.11 (23%)	0.15
1-aTf	534	1.04 (77%), 2.83 (23%)	0.087

Table 6

Cellular uptake and cytotoxicity (IC_{50}, 48 h) of the DIBO complexes and cisplatin toward the CHO cell line.

complex	no. of mole[a]/fmol	IC_{50}/μM
1a	0.32 ± 0.02	9.55 ± 1.55
2a	1.42 ± 0.13	3.50 ± 0.03
3a	2.07 ± 0.06	2.94 ± 0.02
cisplatin	N. A.	25.49 ± 0.54

[a] Numbers of moles of rhenium(I) associated with a typical CHO cell upon incubation with the complexes (10 μM) at 37 °C for 1 h.

Figure and Scheme Captions

Fig. 1. Emission spectra of complexes **1a** (solid line), **2a** (dashed line), and **3a** (dotted line) in CH_3CN at 298 K.

Fig. 2. The k_{obs} values for the reactions of complexes **1a**, **2a**, and **3a** with different concentrations of benzyl azide in MeOH at 298 K.

Fig. 3. Results of SDS-PAGE of complex **1a** (50 μM) incubated with azide-modified and unmodified proteins (BSA, HSA, or aTf, 500 μg protein/mL) for 24 h. Top: UV transillumination; bottom: Coomassie Blue staining. Lane 1: protein ladder; Lanes 2, 5, and 8: unmodified BSA, HSA, aTf, respectively; Lanes 3, 6, and 9: complex **1a** with azide-modified BSA, HSA, aTf, respectively; Lanes 4, 7, and 10: complex **1a** with unmodified BSA, HSA, aTf, respectively

Fig. 4. Laser-scanning confocal microscopy images of CHO cells incubated with complex **1a** (5 μM, 37 ^{o}C, 1 h). Conditions used from left to right: no inhibitors added; with the cytoskeletal inhibitor colchicine (10 μM, 1 h); with the ATPase inhibitor potassium nitrate (50 mM, 1 h); incubation temperature = 4 ^{o}C.

Fig. 5. Imaging of azide-labeled glycans on live cells using complex **1a**. (a) CHO cells were preincubated with (top) or without (bottom) 50 μM Ac_4ManNAz for 72 h. The cells were subsequently treated with 5 μM of complex **1a** at 37 °C for 1 h. (b) The conditions were the same as in (a) except that the cells were treated with complex **1a** for 24 h.

Fig. 6. Relative cellular uptake of rhenium associated with an average CHO cell upon incubation with complex **1a** (5 μM) at 37 ^{o}C for various time. CHO cells were preincubated with (shaded) or without (empty) Ac_4ManNAz (50 μM) at 37 ^{o}C for 72 h. The uptake of the complex in the Ac_4ManNAz-untreated cells at 1-h incubation time

was set as a reference point.

Scheme 1. Structures of the rhenium(I) DIBO complexes **1a** – **3a** and their DIBO-free counterparts complexes **1b** – **3b**.

Scheme 2. Reactions of the DIBO complexes with benzyl azide.

Scheme 3. Bioorthogonal labeling of biomolecules using complex **1a**.

Graphical Abstract

A series of rhenium(I) polypyridine dibenzocyclooctyne (DIBO) complexes was developed as a new class of phosphorescent labels for azide-modified biomolecules. Various experiments revealed that these complexes can specifically react with azide-containing compounds. One of the DIBO complexes was used to image CHO cells pretreated with 1,3,4,6-tetra-*O*-acetyl-*N*-azidoacetyl-D-mannosamine- (Ac_4ManNAz).

Keywords: bioorthogonal; imaging agents; phosphorescence; rhenium; sensors

Fig. 1

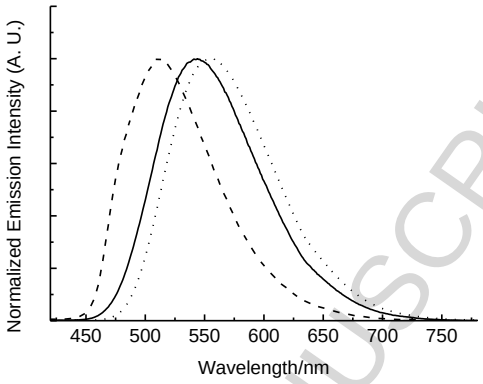

Fig. 2

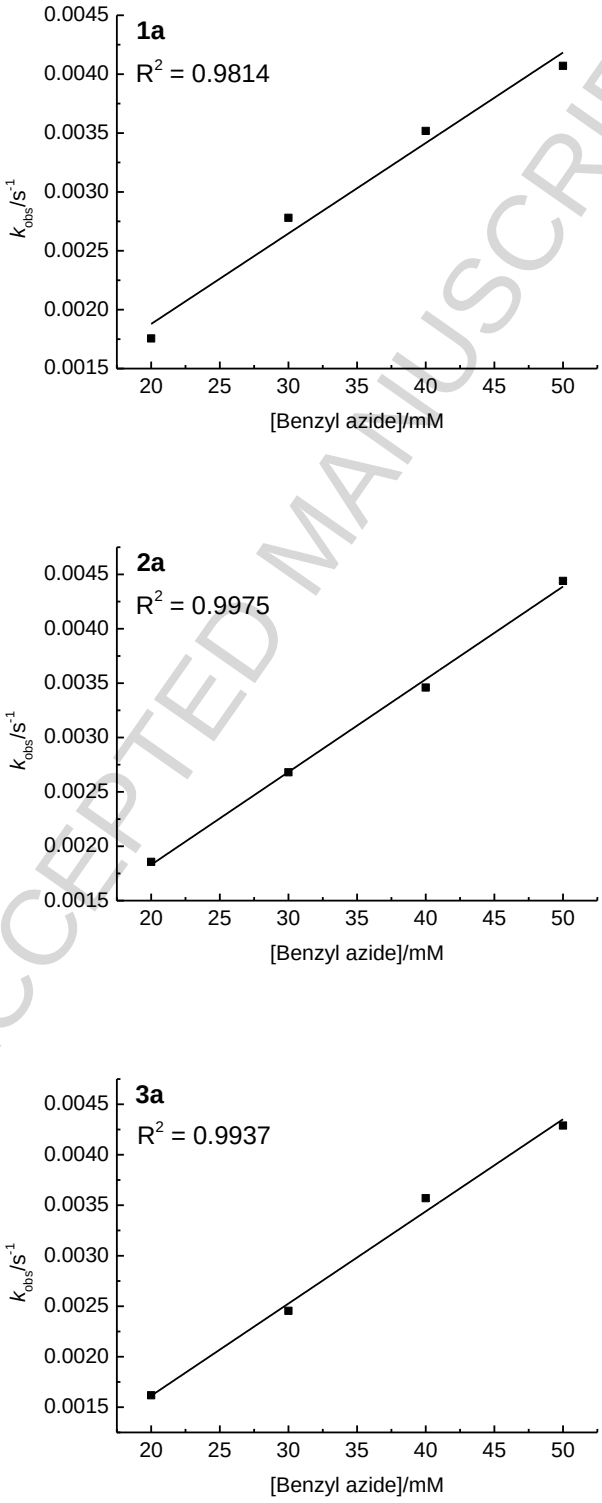

Fig. 3.

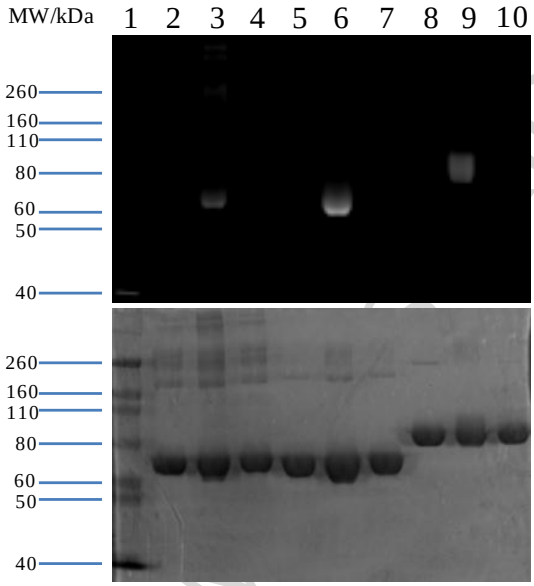

Fig. 4.

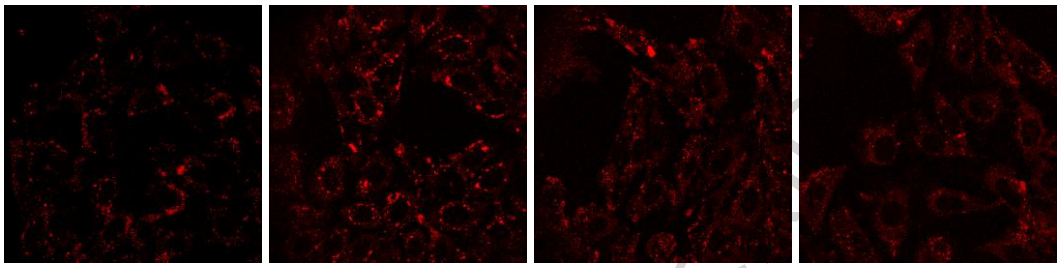

Fig. 5.

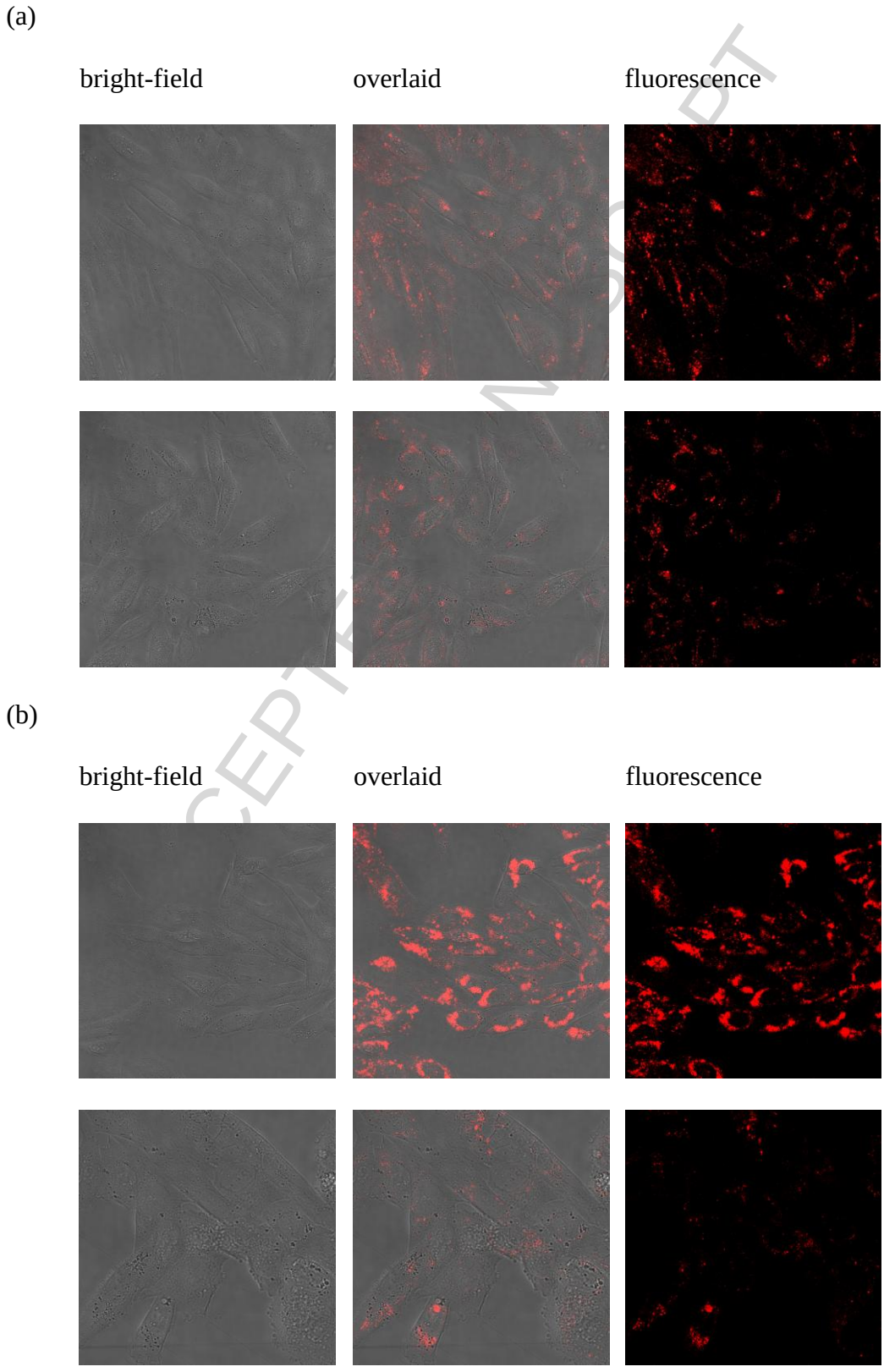

Fig. 6.

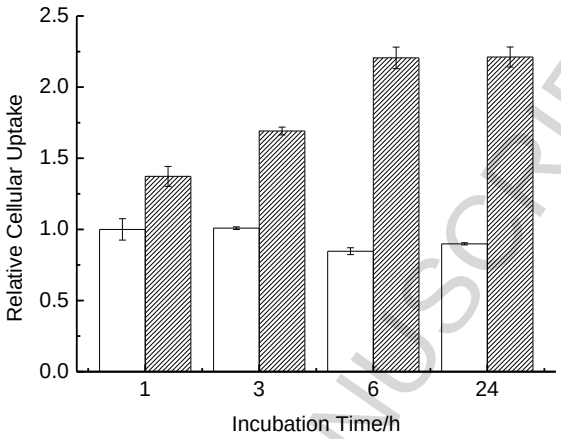

Scheme 1.

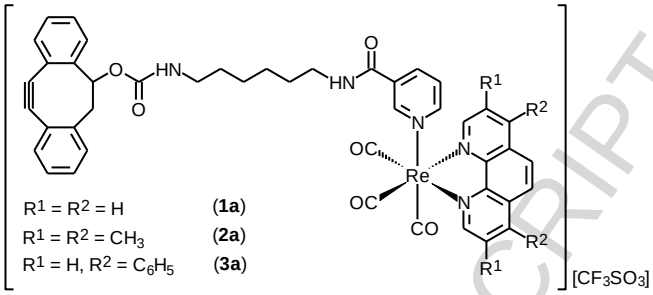

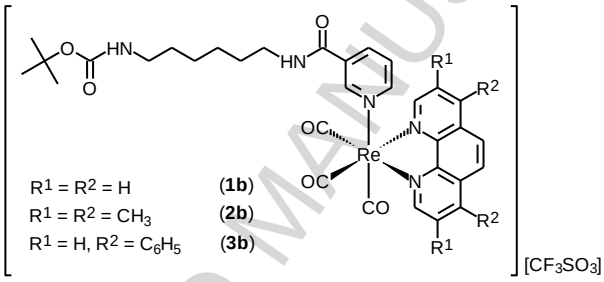

Scheme 2.

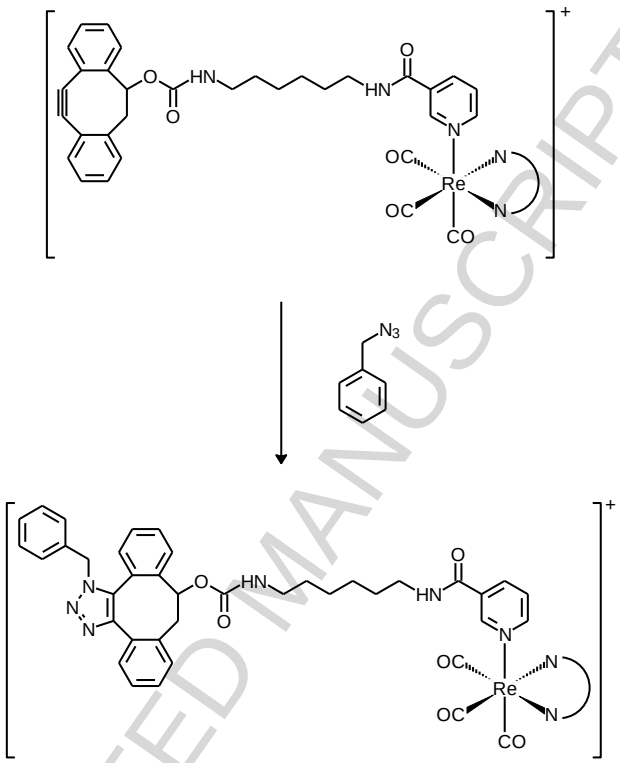

Scheme 3.

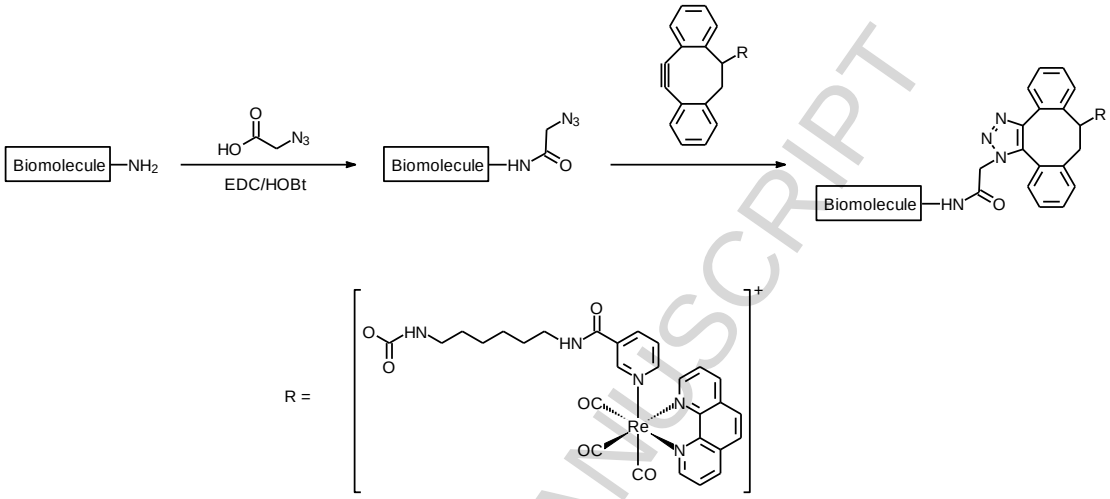

Graphical Abstract

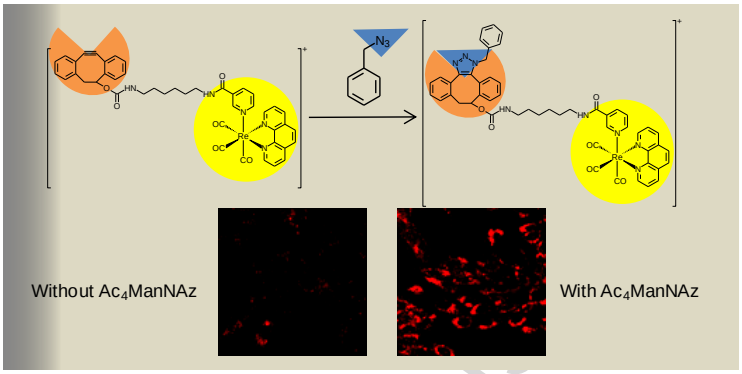

Highlights

- phosphorescent rhenium(I) complexes containing a DIBO unit have been synthesized
- the complexes exhibit interesting photophysical properties and cytotoxic activity
- the complexes undergo facile reactions with azide derivatives
- the complexes serve as bioorthogonal probes for cells treated with Ac_4ManNAz